Vulnerability of soil organic carbon in artificially constructed urban green spaces: Linking soil organic carbon physical fractions, microbial dynamics, and soil properties

Ye Lim Park, You Jin Kim, Jun Ge Hyun, Claire Chenu, Gayoung Yoo

Geoderma 459 (2025) 117364

Contents lists available at ScienceDirect

Geoderma

journal homepage: www.elsevier.com/locate/geoderma

Vulnerability of soil organic carbon in artificially constructed urban green spaces: Linking soil organic carbon physical fractions, microbial dynamics, and soil properties

Ye Lim Park [a], You Jin Kim [b], Jun Ge Hyun [b], Claire Chenu [c], Gayoung Yoo [b,*]

[a] Department of Applied Environmental Science, Kyung Hee University, Yongin, Republic of Korea
[b] Department of Environmental Science and Engineering, Kyung Hee University, 1732, Deogyeong-daero, Giheung-gu, Yongin-si, Gyeonggi-do 446701, Republic of Korea
[c] Université Paris-Saclay, INRAE, AgroParisTech, UMR Ecosys F-91120 Palaiseau, France

ARTICLE INFO

Handling Editor: Dr Cornelia Rumpel

Keywords:
Urban soils
Carbon sequestration
Soil compaction
Soil pH
Glomalin-related soil protein
Microbial enzyme activities

ABSTRACT

Soils in urban green spaces are often artificially constructed and highly disturbed, yet their capacity for long-term carbon (C) sequestration remains underexplored. This study evaluates soil organic C (SOC) content and vulnerability in three types of urban green spaces, tree-only roadside greenery, belt-type roadside greenery, and urban parks, with a natural grasslands serving as a reference. We analyzed SOC physical fractions and microbial activity under varying soil structural and chemical conditions, using the SOC vulnerability index (SOCVI), defined as the ratio of labile to stable fractions, to assess SOC stability. Results show that urban parks and tree-only roadside greenery have 87% lower SOC content than grasslands on average, and they contain a disproportionately high fraction of labile C, which increases SOC vulnerability. Tree-only roadside greenery exhibited particularly high SOCVI primarily because, despite low overall C inputs, its microbial activity relative to SOC is high, leading to inefficient stabilization of SOC as stable fractions. This condition is further exacerbated by alkaline pH and compaction, which hinder effective C sequestration. Although belt-type roadside greenery achieved higher SOC content through additional C inputs from understory vegetation and slightly improved soil structure, its SOCVI remained high, indicating that increased C inputs alone does not ensure stabilization. Structural equation modeling identified that mean annual temperature (MAT), soil pH and glomalin-related soil protein (GRSP) as key regulators of SOCVI. These findings underscore that enhancing SOC sequestration in urban green spaces requires integrated management strategies that optimize soil pH, improve structural properties, and support beneficial microbial activity alongside increased C inputs.

1. Introduction

Urban soils, influenced by rapid urbanization and extensive land-use change, represent a dynamic yet often overlooked carbon (C) reservoir (Meyer and Turner, 1992; Seto et al., 2012). Unlike natural ecosystems, they are subjected to intense anthropogenic pressures such as compaction, pollution, and chemical disturbances that can disrupt their capacity to store and stabilize C (Jim, 1993; Lorenz and Lal, 2009). In urban environments, impervious surfaces dominate, leaving only small patches of exposed soil in areas such as roadside greeneries or parks (Hu et al., 2018). Although these urban soils share certain characteristics, such as compaction and chemical alterations (Jim and Ng, 2018; Scharenbroch and Catania, 2012; Sefati et al., 2019), they exhibit a remarkably wide spectrum of SOC storage. For instance, older, well-maintained urban parks, such as Victoria Park in the United Kingdom, have been reported to accumulate relatively high SOC content (Cambou et al., 2018; Jim, 1998; Pouyat et al., 2006). Even roadside greeneries, typically considered suboptimal for SOC storage (Jim, 1998; Jim and Ng, 2018), may store significant amounts of C if mature and adequately managed (Lorenz and Kandeler, 2005; Zhao et al., 2013).

In contrast, artificially constructed urban green spaces, such as those created during new town construction or major road expansion, often display extremely low SOC contents (Bae and Ryu, 2015; Yoon et al., 2016). These soils were frequently comprised of fill materials or subsoils with minimal organic matter (OM), limiting their initial C storage (Du et al., 2022). Moreover, they are often subject to unsustainable

* Corresponding author at: Department of Environmental Science and Engineering, Kyung Hee University, 1732, Deogyeong-daero, Giheung-gu, Yongin-si, Gyeonggi-do 446701, Republic of Korea.
E-mail address: gayoo@khu.ac.kr (G. Yoo).

https://doi.org/10.1016/j.geoderma.2025.117364
Received 1 March 2025; Received in revised form 1 May 2025; Accepted 21 May 2025
Available online 26 May 2025

management practices, where leaf litter is routinely removed, and human-induced disturbances such as soil compaction, waste disposal, or chemical pollutants (e.g., de-icing agent, concrete) are common. This reliance on imported or heavily disturbed substrates, combined with inadequate maintenance, impedes SOC accumulation and further restricts its stabilization (Jim, 1998; Phillip, 1985; Truscott et al., 2005).

Understanding why artificially constructed urban soils often fail to sequester C effectively requires investigating not just total SOC but also the distribution of SOC fractions. Soil physical fractionation techniques distinguish labile fractions, those that decompose rapidly, from more biogeochemically stable fractions (Balesdent, 1996; Cotrufo et al., 2019; Del Galdo et al., 2003; Six et al., 1998). Previous studies have introduced the concept of SOC vulnerability to evaluate its current status and future stability (Lugato et al., 2021; Poeplau et al., 2017). The SOC vulnerability, the ratio of labile to resistant SOC fractions, can provide insights into the physicochemical properties and long-term storage potential of SOC (Baldock et al., 2018; Baldock et al., 2013; Gray et al., 2019; Viscarra Rossel et al., 2019). However, it may overlook the critical role of microbial activity, which drives SOC decomposition and is strongly influenced by soil structure (e.g., pore space, compaction) and chemical conditions (e.g., pH, pollutants) (Torbert and Wood, 1992; Zhang et al., 2020).

In light of this, a more comprehensive understanding of SOC storage in artificially constructed urban soils requires an in-depth investigation of microbial activity alongside fraction-based assessments. While several studies have reported microbial activity levels in artificially constructed urban soils, few have directly linked microbial data with soil structural and chemical properties to elucidate C sequestration dynamics (Liu et al., 2016). This gap in our understanding hinders the development of targeted solutions for enhancing SOC storage in these soils. Therefore, further research is needed to elucidate how soil physical fractions, microbial processes, and urban soil characteristics, including compaction, chemical alterations, and limited OM inputs, collectively influence SOC storage.

Accordingly, this study aims to clarify the mechanisms underlying low SOC storage in artificially constructed urban soils by integrating SOC physical fractionation analysis and microbial activity assessments under different soil structural (e.g., compaction) and chemical (e.g., pH) conditions. To obtain representative artificially constructed urban soils, we selected urban parks and two types of roadside greenery, which are typical forms of urban green spaces (Korea Forest Service, 2024). Our objective is to understand the physical, microbiological, and chemical factors influencing SOC vulnerability in artificially constructed urban green spaces. Specifically, we hypothesized that (1) SOC vulnerability would be high in artificially constructed urban green spaces due to impaired soil structure and unfavorable chemical conditions, and (2) enhanced C inputs from multi-layer planting in tree-only roadside greenery would not effectively reduce SOC vulnerability unless soil structural and chemical conditions are improved concurrently.

2. Materials and methods

2.1. Site description

This study was conducted in artificially constructed urban green spaces in the Seoul metropolitan area, South Korea, to investigate the SOC vulnerability and its influencing factors. Three representative types of urban green spaces were selected: tree-only roadside greenery, belt-type roadside greenery, and urban parks. These three types of urban green spaces collectively represent typical urban greenery found across the Seoul metropolitan region. According to the Korean Legislation Research Institute (2017), urban green spaces are classified into urban forests, neighborhood forests, and roadside greenery. Among them, urban parks account for 84.4 % of the combined area of urban and neighborhood forests (Korea Forest Service, 2024), highlighting their role as the most representative type of urban green space. In addition to urban parks, two types of urban roadside greenery-tree-only and belt-type-also serve as representative forms of urban green space, with their distribution in the Seoul metropolitan area being nearly equal (Data Science Lab, 2021). All three green space types are located within the same climatic context, specifically the warm temperate, moist climate zone, as defined by the IPCC's Good Practice Guidance for Land Use, Land-Use Change, and Forestry (GPG-LULUCF) (Penman et al., 2003). This region experiences a mean annual temperature (MAT) of 12.2 ± 0.2 °C and annual precipitation of $1,262.8 \pm 7.5$ mm, based on 2011–2020 data from the Korea Meteorological Administration.

This study focused on representative urban green space types distributed within this climatic context, beginning with tree-only roadside greenery. The tree-only roadside greenery, established prior to 2008, included three sampling sites, one in Seoul and two in Suwon (KakaoMap, 2025; Fig. S1). These sampling sites represented the typical roadside greenery configuration in South Korea, where a single tree is planted in a cubic planting pit (width: 1.2–1.6 m, length: 1.0–1.6 m, depth: 0.5–1.0 m) without mulching (Korea Forest Service, 2020). The planting pits were filled with sandy soil mixed with organic fertilizer at a recommended standard rate of approximately 1 kg m^{-2}, when constructed (Korea Forest Service, 2020; National Forestry Cooperative Federation, 2010). However, actual fertilization is restricted to conditions of critically low initial soil OM (<1%) (Korea Forest Service, 2020). Following establishment, maintenance interventions are minimal, usually consisting only of replacing dead trees and conducting essential pruning or pest control (Korea Forest Service, 2020). In this study, *Pinus densiflora* and *Zelkova serrata* were planted in Seoul, whereas only *Zelkova serrata* was planted in Suwon. These species are commonly selected for their aesthetic appeal and resilience to urban environmental stresses, including air pollution and climatic variation in South Korea (Kim and Jung, 2019; Kim and Yoo, 2020).

The second type of urban green space is the belt-type roadside greenery, which comprised trees, shrubs, and herbaceous plants arranged in elongated planting pits (1.2–1.4 m in width, 4.0–26.0 m in length, and 0.5–1.0 m in depth) (Korea Forest Service, 2007). It has been proposed to overcome the limitations of the tree-only configuration, which is characterized by narrow planting pits and heavy soil compaction (Day and Bassuk, 1994). This strategy is expected not only to enhance C sequestration but also to improve various ecosystem services, such as biodiversity and air pollution reduction. The sampling sites of belt-type roadside greenery included two in Seoul and one in Suwon, located adjacent to the sites of tree-only roadside greenery, to assess its impact on SOC sequestration (Fig. S1, S2). When belt-type roadside greenery constructed, soil management practices for planting pits were identical to those for tree-only roadside greenery, except that organic fertilizer was applied at different rates: 1.0 kg m^{-2} for trees and 0.5 kg m^{-2} for shrubs (Korea Forest Service, 2020; National Forestry Cooperative Federation, 2010). The belt-type roadside greenery consisted of *Pinus densiflora* and *Zelkova serrata* as upper canopy trees, with *Ligustrum obtusifolium* and *Euonymus japonicus* as understory shrubs. Trees were evenly spaced, and shrubs occupied the gaps between trees.

The third type of urban green space, urban parks, included three sampling sites: Maeheon Citizen's Forest Park and Dream Park in Seoul, and Children Transportation Park in Suwon. These parks were established in 1986, 2009, and 1998, respectively, selected to represent spatial variability across the northern, central, and southern Seoul metropolitan area (Fig. S3). These parks are actively managed urban forests, artificially designed and planted with trees, shrubs, and herbaceous vegetation, rather than extensions of natural forest areas. At the time of park construction, the soil consisted of sandy loam containing less than 1 % OM, imported from external sources and applied as topsoil. The soil was subsequently tilled to a depth of 30 cm using a rotary tiller (Korea Forest Service, 2007). The vegetation structure of these parks was established according to the national landscaping plan ("Act on Urban Parks and Green Areas, etc.," 2005). Dominant species included *Ginkgo biloba*, *Pinus densiflora*, *Zelkova serrata*, and *Metasequoia* *glyptostroboides* for tree; *Spiraea prunifolia simpliciflora*, *Rhododendron indicum*, and *Euonymus japonicus* for shrubs; and *Zoysia japonica*, *Liriope muscari*, *and Trifoloum repens* for grasses (Korea Forest Service, 2007). Management practices at these sites included regular replacement of dead or damaged plants, pruning primarily during the dormant season (February-March), pest control, litter removal, and annual application of organic fertilizer at a recommended total rate of 2–3 kg m^{-2} in early spring (Suwon City, 2018).

As a reference to evaluate SOC dynamics in urban green spaces, grasslands in Gangwon-do, South Korea, were selected (Fig. S4). Since grasslands maintained for over 20 years without significant disturbance do not exist on the outskirts of Seoul metropolitan area, it is difficult to observe minimally disturbed SOC sequestration processes within the immediate urban surroundings. Therefore, this study employed a geographically distant grasslands site with comparable edaphic and climatic conditions, assuming that SOC stabilization processes at this site were sufficiently representative of natural conditions (Ministry of Land, 2020). The grasslands included three sampling sites in Pyeongchang and Taebaek, predominantly composed of temperate perennial grasses, including *Trifolium repens* (white clover) and *Dactylis glomerata* (orchard grass). Unlike artificially constructed urban green spaces, the grasslands allowed plant residues and livestock manure to remain undisturbed, facilitating natural C cycling and enhancing soil structure (Liang et al., 2021). Additionally, nominal management practices, such as controlled NPK fertilizer application (28–20-24 kg ha^{-1} yr^{-1}), annual overseeding of perennial grasses, and grazing without mowing, were employed to support plant growth while minimizing soil disturbance (Seo, 1992).

2.2. Soil sampling

Soil samples were collected from a 0–15 cm depth, where the C sequestration process is most dynamic. The sampling dates varied slightly between urban and grasslands sites; urban soil samples were collected in May 2019–2021, whereas grasslands soil samples were collected between August and early October 2020–2021, coinciding with the peak growing season for grasslands. Three samples were taken at each three sampling points across all green space types. Soil samples were collected using a split-core sampler (2.5 cm diameter, 35 cm length; AMS Inc., USA) for the grasslands and urban parks (classified as Inceptisols), and a soil auger (1.3 cm diameter, 48 cm length; PHYWE, Germany) for the tree-only and belt-type roadside greeneries, which are classified as Technosols (Group, 2014; National Geographic Information Institutem, 2020). Half of each sample was air-dried for two weeks, sieved to < 2 mm, and prepared for physical, chemical, and microbial analyses (i.e., glomalin-related soil protein and basal respiration). The remaining samples were frozen at −20°C and stored for microbial extracellular enzyme activity analysis.

2.3. Soil analysis

2.3.1. Soil physicochemical analysis

Soil texture was determined using the hydrometer method (Chen et al., 2015). Soil pH was measured at a 1:5 (w/v) soil-to-deionized water ratio using a pH meter (Orion 3 star, Thermo Fisher Scientific, USA). To assess soil compaction, we measured bulk density and total pore volume. Bulk density of grasslands soils was directly measured using core sampling (core 10 cm diameter; 2″ x 12″ Soil Core Sampler Complete, AMS, American Falls, ID, USA). However, core sampling in urban soils was not feasible due to severe compaction and the presence of artificial materials. Instead, bulk density for urban soils was indirectly estimated from penetrometer resistance (PR) values and soil depth (*d*) of PR measurements using push-cone (DIK-5553, Daiki Rika Kogyo Co., Ltd., Saitama, Japan), following the approach of Hernanz et al. (2000):

$$Bulk\ density\ \left(g\ cm^{-3}\right) = 0.913 \times PR^{0.096} \times d^{-0.06}$$

Total pore volume was measured using the WP4C Dewpoint Potentiometer (METER Group, Inc., Pullman, WA, USA). The total pore volume was calculated based on a water retention curve generated from the relationship between matric potential (kPa) and volumetric water content (VWC), with the VWC at 0 kPa representing the fully saturated state of the soil (Kim et al., 2021a). To examine whether contamination by potentially toxic elements (PTEs; Cu, Pb, Zn, Ni, Cd, and Cr) influenced SOC stability, we extracted soil samples (5 g each) with 25 mL of 0.1 N HCl solution and analyzed the extracts using inductively coupled plasma mass spectrometry (ICP-MS; Agilent 7500cx, Agilent Technologies, Santa Clara, CA, USA).

SOC content was analyzed using the following procedures: first, total C (TC) was measured using an elemental analyzer (EA; FlashEA 1112, Thermo Fisher Scientific, Waltham, MA, USA). Next, inorganic C (IC) was removed by acid washing with 1 M HCl (Midwood and Boutton, 1998). The IC-free sample was subjected to thermal gravimetric analysis (TGA) to quantify the relative proportions of organic C (OC) and black C (BC) based on weight loss at 200–470 °C and 470–600 °C, respectively (Edmondson et al., 2015). Finally, the corrected OC and BC proportions were applied to the C content of the IC-free sample to calculate the SOC content.

2.3.2. SOC fractionation

Soil fraction was conducted using a density-size fractionation method to classify C pools into labile and stable fractions (Fang et al., 2019). A 20 g sample of air-dried soil was mixed with 1.6 g cm^{-3} sodium polytungstate (SPT) solution, dispersed at 60 rpm. The material floating in the supernatant was designated as free particulate organic C (fPOC). The remaining precipitate was dispersed at 300 rpm with distilled water and glass beads, then wet-sieved through a 53 μm sieve. Particles larger than 53 μm were classified as occluded particulate organic C (oPOC), while smaller particles were designated as mineral-associated organic C (MAOC). After fractionation, each sample was repeatedly washed with distilled water and oven-dried at 60℃. The fractionation process achieved a weight recovery rate of 100.8 ± 1.0 %, ensuring minimal loss of soil material and high reliability. We determined all fractions' C concentration (C%) using an elemental analyzer (EA; FlashEA 1112, Thermo Fisher Scientific, Waltham, MA, USA). Subsequently, the relative weight proportion of each fraction was calculated as the fraction weight divided by the total weight of the bulk soil sample. Each fraction's C content (g C kg $soil^{-1}$) was then calculated by multiplying its relative weight proportion by the total SOC content of the bulk soil, with SOC recovery rate of 97.0 ± 6.3 % on average. For oPOC and MAOC, the proportion of IC was subtracted from the calculated C content to ensure that only OC was accounted for in these fractions, aligning with the study's focus on SOC dynamics.

2.3.3. Soil microbial analysis

We analyzed glomalin-related soil protein (GRSP), a glycoprotein produced by arbuscular mycorrhizal fungi that enhances soil aggregate stability by binding SOC, roots, microbes, and mineral particles (Rillig, 2004; Wright and Upadhyaya, 1998). GRSP was extracted using 50 mM sodium citrate solution (pH 8) following Wright and Upadhyaya (1998), with repeated autoclaving at 121℃ for 30 min and centrifugation at 10,000 x *g* for 10 min until the supernatant was clear. Its content was quantified using the Bradford protein assay with bovine serum albumin (BSA) as a standard, and absorbance was measured with a multifunctional microplate reader (FLUOstar Omega, BMG LABTECH, Germany).

Basal respiration (BR), reflecting the natural microbial decomposition of OM, was measured without the addition of external substrates. Soil samples (50 g dry weight equivalent) were placed in 280 mL flask and incubated at 25 °C in the dark for 8 days, with soil moisture adjusted to 50 % water-filled pore space, representing optimal conditions for microbial activity (Franzluebbers, 2020; Jian et al., 2020). Gas samples were collected daily from the headspace through a rubber septum using a gas-tight syringe, following 15 min equilibration period and thorough mixing by pumping the syringe five times before sampling. The collected gas samples were immediately analyzed for CO_2 fluxes using gas chromatography (Agilent 7890A, USA) equipped with a thermal conductivity detector (TCD) (Troy et al., 2013). The CO_2 flux was calculated as:

$$CO_2 \text{ flux } \left(gCO_2\, kg\, soil^{-1} day^{-1}\right) = \frac{dGas}{\text{dt}} \times \frac{V}{A} \times \frac{(P \times 100 \times MW)}{R} \times \frac{293}{T} \quad (1)$$

where $\frac{dGas}{dt}$ represents the change in CO_2 concentration before and after 40 min incubation period, V and A denote the volume and area of the incubation bottle, respectively. P is the atmospheric pressure (1 atm), MW is the molecular weight of CO_2 (44.01 g mol^{-1}), R is the gas constant (0.082 atm L mol^{-1} K^{-1}), and T is the absolute temperature during gas collection (293 K). The daily CO_2 flux measurements were averaged over the 8 days incubation period to calculate the BR. To standardize microbial activities across the four green spaces, each BR was normalized by dividing by the SOC content to calculate the specific BR ($BR_{specific}$).

Extracellular enzyme activities were measured to evaluate microbial enzyme activities under substrate-saturated conditions. To ensure accurate enzyme activity measurements, soil samples were extracted with acetate buffer to maintain pH stability during the assays, and substrates were added in excess to eliminate substrate limitations. The reactions were incubated at a controlled temperature of 25 °C. Hydrolase (HY) activity, β-1,4-glucosidase, was determined using a fluorometric assay with 4-MUF β-D-glucopyranoside as the substrate, with an incubation time of 60 min. Oxidase (OX) activity, phenol oxidase, was assessed by measuring the oxidation of L-3,4-dihydroxyphenylalanine (L-DOPA) at 460 nm, following 15 min of incubation. Absorbance readings were obtained using a multifunctional microplate reader (FLUOstar Omega, BMG LABTECH, Germany) (Dunn et al., 2014; Saraswati et al., 2016). HY activity, such as β-1,4-glucosidase, indicates the microbial decomposition of labile C pools, whereas OX activity, including phenol oxidase, is associated with the degradation of recalcitrant C. By analyzing both enzyme activities, we obtained complementary insights into the microbial processes governing SOC stability. To standardize microbial activities across the four green spaces, each enzyme activity was normalized by dividing by the SOC content to calculate the specific enzyme activity ($HY_{specific}$, $OX_{specific}$).

2.3.4. SOC vulnerability index (SOCVI)

The SOC vulnerability index (SOCVI) is a quantitative metric derived from the relative proportions of fPOC, oPOC, and MAOC, representing the stability of SOC against decomposition (Baldock et al., 2018; Viscarra Rossel et al., 2019). A higher SOCVI signifies decreased SOC stability, suggesting it more susceptible to decomposition. The SOCVI was calculated based on the C distribution across all fractions using the following equation:

$$SOC\ vulnerability\ index\ (SOCVI) = \frac{SOC_{fPOC}}{SOC_{oPOC} + SOC_{MAOC}} \quad (2)$$

where SOC_{fPOC}, SOC_{oPOC}, and SOC_{MAOC} represent the contents of fPOC, oPOC, and MAOC, respectively.

2.4. Statistical analysis

Analysis of variance (ANOVA) was performed using the GLM procedure in SAS 9.4 (SAS Institute Inc., Cary, NC, USA) to compare the measurement data among the grasslands, the urban parks, and the tree-only roadside greenery. The Least significant difference (LSD) was employed as a post-hoc analysis to identify significant differences among these three green space types. Statistical significance was evaluated at $p < 0.05$, while statistical tendencies were considered for $p < 0.10$. Pearson's correlation analysis was conducted using the CORR procedure (SAS 9.4) to examine relationships between SOCVI and climate, soil physicochemical and microbial parameters. Subsequently, the structural equation model (SEM) was employed to identify the significant pathways by which soil physicochemical properties and microbial variables influenced SOCVI in artificially constructed urban green spaces. This analysis was conducted using the "lavaan" package in RStudio 4.2.1 (Posit, Boston, MA, USA). Based on the ANOVA and correlation analyses, an initial hypothetical model was constructed to encompass all plausible interaction pathways from the soil physicochemical and microbial variables to SOCVI, which was further refined using SEM techniques (Kim and Yoo, 2020). For model evaluation and selection, the chi-square (χ^2) test, root mean squared error of approximation (RMSEA), goodness-of-fit index (GFI), and comparative fit index (CFI) were used to examine whether the estimated pathways adequately fit the data (Yang et al., 2022; Zhang et al., 2019a). Larger χ^2 values are better, and a χ^2 p-value > 0.05 indicates a better fit. The RMSEA < 0.05 and < 0.10 indicate perfect and foot fits of the model, respectively. The GFI and CFI values > 0.90 indicate a good (Tabachenik and Fidel, 2012).

3. Results

3.1. Soil physicochemical properties

Soil texture was classified as sandy loam in the grasslands and the urban parks, whereas loamy sand in the two types of roadside greenery (Table 1). The clay content in the grasslands (10.4 ± 1.0 %, mean ± standard error) was similar to that in the urban parks (10.8 ± 1.0 %), and both were significantly higher than that in the tree-only roadside greenery (5.3 ± 0.9 %) and belt-type roadside greenery (5.3 ± 1.6 %). The soil pH was lowest in the grasslands (5.3 ± 0.1), followed by the urban parks (6.1 ± 0.3), belt-type roadside greenery (6.3 ± 0.1), and highest in the tree-only roadside greenery (7.7 ± 0.1). The bulk density was lowest in the grasslands (0.74 ± 0.04 g cm^{-3}), followed by urban parks (1.00 ± 0.08 g cm^{-3}), belt-type roadside greenery (1.51 ± 0.03 g cm^{-3}), and highest in the tree-only roadside greenery (1.62 ± 0.03 g cm^{-3}). Conversely, the total pore volume was highest in the grasslands (67.9 ± 1.9 %), followed by the urban parks (57.5 ± 4.3 %), belt-type roadside greenery (15.3 ± 1.9 %), and lowest in the tree-only roadside greenery (11.3 ± 1.6 %). The concentrations of PTEs (Cu, Pb, Zn, Ni, Cd, and Cr) at all study sites were below the permissible limits suggested by

Table 1
Climate and basic physicochemical properties of soils across the grasslands, urban parks, and tree-only and belt-type roadside greeneries (n = 36). Alphabets within rows indicate significant differences among the green space type (ANOVA, $p < 0.05$).

Green space type	Grassland	Urban park	Roadside greenery	
			Tree-only	Belt-type
Mean annual temperature (°C)	9.90 ± 0.15^A	12.93 ± 0.03^B	12.87 ± 0.03^B	12.93 ± 0.03^B
Soil texture	Sandy loam	Sandy loam	Loamy sand	Loamy sand
Clay (%)	10.44 ± 0.97^B	10.78 ± 1.90^B	5.28 ± 0.88^A	5.28 ± 1.58^A
pH	5.34 ± 0.08^A	6.09 ± 0.27^B	7.66 ± 0.11^C	6.25 ± 0.14^B
Bulk density† (g cm^{-3})	0.74 ± 0.04^A	1.00 ± 0.08^B	1.62 ± 0.03^D	1.51 ± 0.03^C
Total pore volume‡ (%)	67.90 ± 1.93^C	57.47 ± 4.30^B	11.26 ± 1.57^A	15.28 ± 1.91^A
GRSP (mg g $soil^{-1}$)	10.94 ± 0.67^C	4.29 ± 0.43^B	2.36 ± 0.17^A	3.53 ± 0.28^{AB}

† Bulk density was measured using a split-core sampler (2.5 cm diameter, 35 cm length; AMS Inc., USA) for the grasslands and urban parks (classified as Inceptisols), and a soil auger (1.3 cm diameter, 48 cm length; PHYWE, Germany) for the tree-only and belt-type roadside greeneries.
‡ GRSP; glomalin-related soil protein.

South Korean Soil Contamination Warning Standards (SCWS, Area 1) and the United States Environmental Protection Agency (US EPA) soil screening levels (US EPA, 2021), confirming that contamination by these elements did not significantly influence SOC stability (Table S1).

3.2. SOC content and fractionation

The SOC content in the grasslands (36.0 ± 4.4 g C kg soil^{-1}) was significantly higher in the grasslands compared to the urban parks (6.3 ± 0.7 g C kg soil^{-1}) and belt-type roadside greenery (8.3 ± 1.6 g C kg soil^{-1}), and lowest in the tree-only roadside greenery (3.1 ± 0.6 g C kg soil^{-1}) (Fig. 1). Furthermore, the distribution of SOC fractions varied across the green space types. The labile SOC fraction, fPOC, was lowest in the grasslands (17.7 ± 1.4 % of SOC), followed by the urban parks (22.9 ± 2.9 % of SOC) and belt-type roadside greenery (48.7 ± 10.6 % of SOC), and highest in the tree-only roadside greenery (58.0 ± 6.6 % of SOC). Conversely, the stable SOC fractions, oPOC and MAOC, accounted for the most considerable proportions in the grasslands (53.2 ± 2.7 % and 29.1 ± 3.0 % of SOC, respectively) and the urban parks (52.4 ± 4.3 % and 24.7 ± 4.0 % of SOC, respectively), while they were lower in the belt-type (36.4 ± 8.0 % and 14.9 ± 4.4 % of SOC, respectively) and tree-only roadside greenery (28.4 ± 4.0 % and 13.6 ± 3.7 % of SOC, respectively).

3.3. Soil microbial properties

Soil microbial properties differed significantly among the green space types (Fig. 2). The GRSP content was highest in the grasslands (10.6 ± 0.7 mg g^{-1} soil), followed by the urban parks (4.3 ± 0.4 mg g^{-1} soil) and belt-type roadside greenery (3.5 ± 0.3 mg g^{-1} soil), and was lowest in the tree-only roadside greenery (2.4 ± 0.2 mg g^{-1} soil; Table 1). Similarly, basal respiration (BR) and hydrolase (HY) activities were significantly higher in the grasslands than in the urban parks and tree-only roadside greenery, between which no significant difference was observed. The belt-type roadside greenery exhibited slightly elevated values relative to the latter two types (Fig. 2a-b).

In contrast, specific microbial activities ($BR_{specific}$, $HY_{specific}$, and $OX_{specific}$) followed a distinctly different pattern, with the highest values consistently observed in the tree-only roadside greenery across all three indicators (Fig. 2d-f). While $BR_{specific}$ did not differ significantly among the other green space types, $HY_{specific}$ and $OX_{specific}$ were notably lower in the grasslands compared to both the urban parks and belt-type roadside greenery. These findings suggest that microbial mineralization efficiency per unit organic C is markedly suppressed in the grasslands, particularly for hydrolytic and oxidative enzymatic functions.

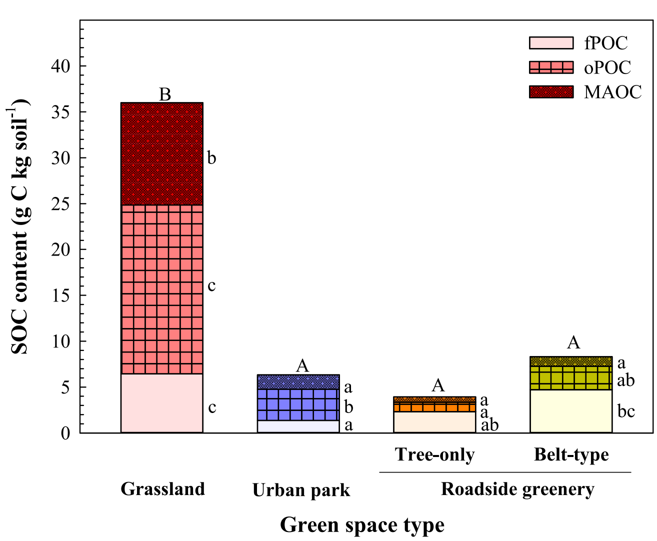

Fig. 1. Soil organic carbon (SOC) content across different green space types. SOC content is partitioned into three fractions: free particulate organic carbon (fPOC; plain), occluded particulate organic carbon (oPOC; checked), and mineral-associated organic carbon (MAOC; dotted). Uppercase letters indicate significant differences in total SOC content, while lowercase letters denote significant differences in SOC fractions (fPOC, oPOC, or MAOC) among grassland, urban park, and tree-only roadside greenery, as determined by ANOVA ($p < 0.05$). (For interpretation of the references to colour in this figure legend, the reader is referred to the web version of this article.)

3.4. SOC vulnerability index (SOCVI) and influencing factors

The SOCVI varied considerably among the different types of urban green spaces, with the highest values observed in the tree-only roadside greenery and the lowest in the grasslands (Fig. 3). The SOCVI in urban parks was comparable to that in the grasslands, whereas the belt-type roadside greenery, despite its higher SOC content, showed no significant difference in SOCVI compared to the tree-only roadside greenery.

Correlation analysis showed that SOCVI was positively associated with mean annual temperature (MAT), soil pH, and specific microbial activities ($BR_{specific}$, $HY_{specific}$, and $OX_{specific}$), but negatively associated with total pore volume and GRSP content (Fig. S4). To further clarify these relationships, structural equation modeling (SEM) was employed. The SEM identified two major pathways linking climate, soil conditions, microbial traits, and SOCVI, explaining 29.8 % of its variance (R^2 = 0.298). The model indicated that MAT, soil pH, total pore volume, $HY_{specific}$, $OX_{specific}$, and GRSP content were the most influential factors, and exhibited a good model fit (χ^2 p = 0.281, RMSEA = 0.079, GFI = 0.993, CFI = 0.991) (Fig. 4).

4. Discussion

4.1. Why is SOC vulnerability extremely high in tree-only roadside greenery?

The extremely high SOCVI observed in tree-only roadside greenery (Fig. 3) highlights severe soil degradation characterized by very low total SOC content and a particularly small fraction of SOC associated with aggregates and minerals. Consistent with our first hypothesis, impaired soil physical structure and unfavorable soil chemical conditions primarily explained this high SOCVI.

From a physical perspective, these soils exhibited extremely high bulk density and very low total pore volume (Table 1), conditions that restrict microbial biomass and suppress overall microbial activities, including BR, HY, OX, and GRSP production (Fig. 2a-c). Such conditions are likely the result of severe soil compaction, driven by frequent vehicular traffic, pedestrian activities, heavy construction equipment use, and coarse textured backfill materials during initial site preparation, especially given the proximity of planting pits to roads (Jim, 1998; Lorenz and Lal, 2009; Scharenbroch et al., 2005). Despite these constraints on total microbial activity, microbial communities in these soils demonstrate notably high specific activity levels ($BR_{specific}$, $HY_{specific}$, $OX_{specific}$; Fig. 2d-f), reflecting their reliance on limited but readily available fPOC inputs. Consequently, this pattern of microbial activity results in the rapid consumption of fPOC rather than its stabilization into more persistent SOC fractions (oPOC and MAOC), further exacerbating SOC vulnerability.

From a chemical perspective, conditions in tree-only roadside greenery further aggravate this highly exploitative C dynamic. Soils located adjacent to impervious road surfaces continuously receive alkaline construction backfill materials and seasonal applications of de-icing agents, resulting in significantly elevated soil pH (Table 1). Such alkaline conditions enhance OX activity, accelerating microbial decomposition of recalcitrant OM. According to Freeman et al. (2001), recalcitrant OM typically suppresses HY activities, thereby stabilizing soil C stocks that a mechanism termed the “enzyme latch hypothesis”. Increased OX activity associated with elevated pH can disrupt this latch,

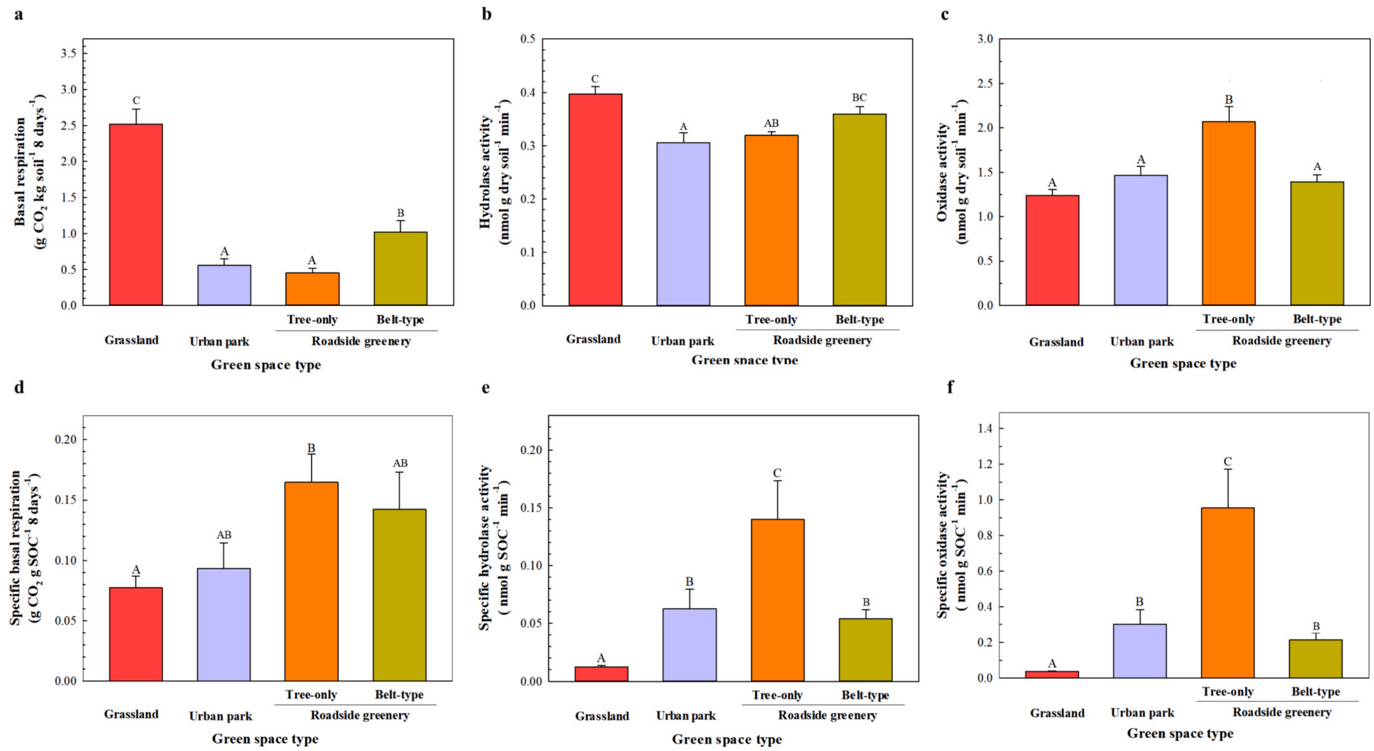

Fig. 2. Soil microbial activities and their specific activities across different green space types. (a) Basal respiration (g CO_2 kg^{-1} soil 8 $days^{-1}$), (b) hydrolase (HY) activity (mmol g^{-1} dry soil min^{-1}), and (c) oxidase (OX) activity (mmol g^{-1} dry soil min^{-1}) are shown for grassland, urban park, and tree-only and belt-type roadside greeneries. (d) Specific basal respiration ($BR_{specific}$; g CO_2 g^{-1} SOC 8 $days^{-1}$), (e) specific hydrolase activity ($HY_{specific}$; mmol g^{-1} SOC min^{-1}), and (f) specific oxidase activity ($OX_{specific}$; mmol g^{-1} SOC min^{-1}) are also presented. Bars represent mean standard errors. Different uppercase letters above bars indicate significant differences among green space types based on ANOVA ($p < 0.05$). (For interpretation of the references to colour in this figure legend, the reader is referred to the web version of this article.)

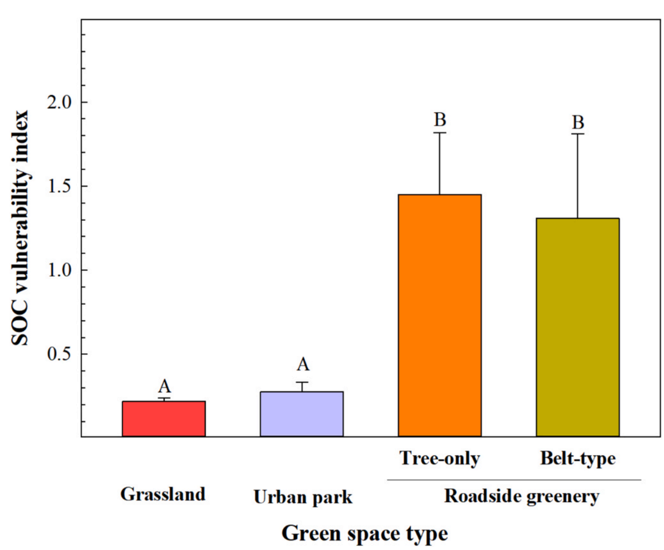

Fig. 3. SOC vulnerability index (SOCVI) across different green space types. Different uppercase letters above the bars indicate significant differences among grassland, urban park, and tree-only roadside greenery based on ANOVA ($p < 0.05$). (For interpretation of the references to colour in this figure legend, the reader is referred to the web version of this article.)

initiating decomposition of recalcitrant OM and consequently activating HY. Although initially identified in wetland soils, recent studies have extended this hypothesis to dry and agricultural soils (Freeman et al., 2001; Kim et al., 2021b; Min et al., 2015; Saraswati et al., 2016; Stursova and Sinsabaugh, 2008). Our results strongly support this enzyme latch hypothesis, emphasizing that minimal organic inputs into tree-only roadside greenery soils are quickly decomposed rather than stabilized.

Additionally, the elevated specific microbial activities observed in tree-only roadside greenery could also be related to the higher MAT typical of urban environments (Delgado-Baquerizo et al., 2023). However, since similarly high MAT conditions apply to urban parks and belt-type roadside greenery, the exceptionally high SOCVI in tree-only roadside greenery underscores that impaired soil physical structure and chemical conditions predominantly drive this heightened SOCVI.

4.2. Can belt-type roadside greenery reduce SOC vulnerability?

Belt-type roadside greenery, characterized by multi-layer vegetation consisting of trees and numerous shrubs, introduces substantially greater organic inputs via roots and leaf litter compared to tree-only roadside greenery (Jeong et al., 2024; Pan et al., 2018). Consequently, SOC content in belt-type roadside greenery was significantly higher (approximately two-fold; Fig. 1). These additional C inputs increased the labile C fraction (fPOC) roughly threefold compared to tree-only roadside greenery, subsequently enhancing overall microbial activities (BR and HY; Fig. 2a-b). Additionally, the belt-type roadside greenery slightly improved soil structure, as evidenced by higher total pore volume and GRSP contents compared to tree-only roadside greenery (Table 1). These structural improvements physically protected labile C fractions, significantly reducing specific hydrolase and oxidase activities (Fig. 2e-f). Nonetheless, structural improvements remained relatively modest, resulting in only a 10 % increase in the proportion of oPOC relative to total SOC compared to tree-only roadside greenery, and no meaningful increase in the MAOC (14.6 % in tree-only vs. 14.9 % in belt-type; Fig. 1). Ultimately, these incremental improvements did not translate into a significant reduction of SOCVI (Fig. 3).

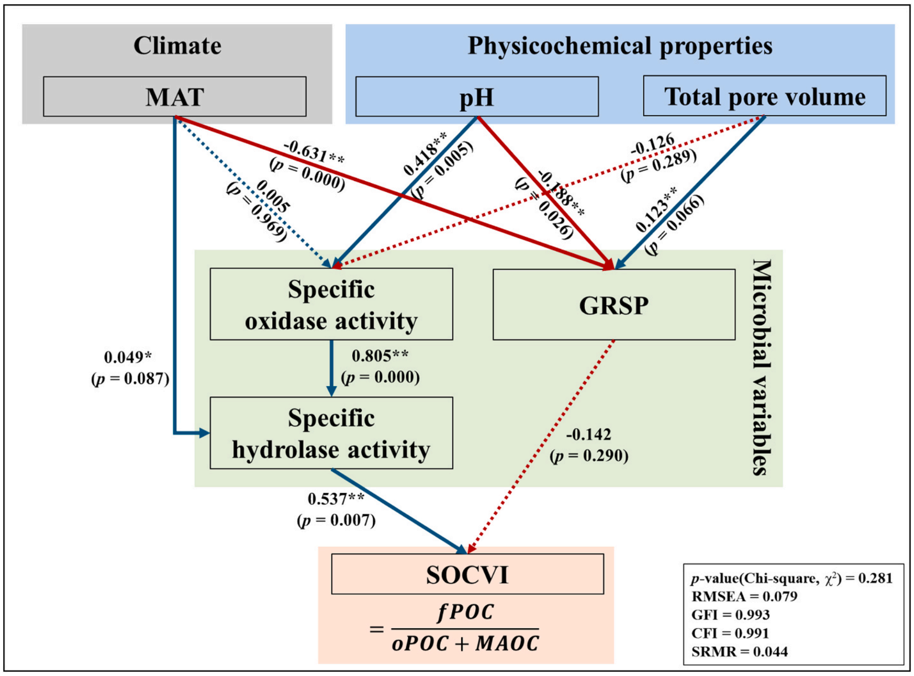

Fig. 4. The structural equation model (SEM) analysis represents the multivariate relationships influencing the SOC vulnerability index (SOCVI) across green space types (tree-only and belt-type roadside greeneries, urban parks, and grasslands). The model highlights pathways through which factors such as climate (mean annual temperature, MAT), soil physicochemical properties (pH and total pore volume) and microbial activity (specific hydrolase activity, specific oxidase activity, and glomalin-related soil protein; GRSP) interact to influence the SOC vulnerability index. The red one-way arrow represents a negative effect, while blue one-way arrows indicate positive effects. The numbers after the arrows represent standardized path coefficients, and the *p*-values are shown in parentheses beneath the path coefficients. The solid arrows represent significant relationships ($p < 0.05$ for '**', $p < 0.10$ for '*'). Dashed arrows represent nonsignificant relationships ($p \geq 0.10$). (For interpretation of the references to colour in this figure legend, the reader is referred to the web version of this article.)

On the other hand, soil pH was notably lower in belt-type roadside greenery (6.25) compared to tree-only roadside greenery (7.66), possibly due to the buffering effect of shrub layers preventing direct infiltration of alkaline de-icing agents into the soil (Miron et al., 2022). Consequently, OX activity levels in belt-type roadside greenery soils remained closer to those observed in urban parks and grasslands, reducing the intensity of C exploitation compared to tree-only roadside greenery. Despite improvements in C inputs and soil chemical conditions, the overall SOCVI remained relatively high, supporting our second hypothesis that increased C inputs alone cannot substantially enhance SOC stability without concurrently improving soil structure.

4.3. Does lower SOC vulnerability in constructed urban parks lead to long-term SOC sequestration?

Although urban park soils experienced less anthropogenic disturbance compared to tree-only and belt-type roadside greenery soils, the artificially constructed urban parks investigated in our study showed limited SOC sequestration, despite having been established for more than 17 years. The SOC content of these urban parks was approximately 25 % of that observed in grasslands and also lower than levels typically reported for mature urban parks in previous studies (Ghosh et al., 2016; Jim, 1998; Pouyat et al., 2006; Scharenbroch et al., 2005). Indeed, their SOC content closely resembled that of the belt-type roadside greenery in this study.

However, the distribution of SOC physical fractions differed significantly between urban parks and belt-type roadside greenery. The relatively low proportion of fPOC observed in urban parks likely results from the current management practice of routinely removing plant residues from the soil surface for aesthetic purposes, combined with the subsequent transformation of remaining fPOC into more stable fractions (oPOC and MAOC). This interpretation is supported by the substantially higher proportions of oPOC and MAOC in urban park soils compared to both tree-only and belt-type roadside greenery soils (Fig. 1). Specifically, the proportion of physically protected oPOC in urban parks (52.4 %) was nearly twice that observed in tree-only roadside greenery (22.9 %), while the proportion of stable MAOC was approximately 65 % greater than that found in belt-type roadside greenery (Fig. 1). These findings suggest more effective stabilization of labile SOC through physical protection mechanisms, consistent with the lower specific basal respiration, higher GRSP content (Table 1), and significantly reduced SOCVI observed in urban parks relative to two types of roadside greenery (Fig. 3).

Despite their relatively low SOCVI, urban park soils still exhibited considerably lower total SOC content compared to natural grasslands, indicating that current management practices are insufficient for achieving robust, long-term SOC sequestration. According to municipal park management guidelines (Suwon City, 2018), current practices primarily involve periodic applications of chemical fertilizers, limited use of organic amendments, and negligible structural improvements. Thus, active management strategies aimed at enhancing SOC sequestration in urban parks should include increased organic amendments, retention of leaf litter, and structural improvements such as biochar addition to effectively promote soil aggregation, microbial activity, and ultimately SOC stability.

4.4. Integrated conceptual diagram for SOC sequestration in urban green spaces

Our structural equation modeling (SEM; Fig. 4) synthesized critical drivers regulating SOCVI in artificially constructed urban green spaces, highlighting climate (MAT), soil chemical properties (pH), and soil physical structure (total pore volume) as key factors controlling microbial activities. Elevated MAT and soil pH notably increased OX and HY activities, which strongly correlated with higher SOCVI. Conversely, higher total pore volume positively influenced GRSP content, which negatively correlated with SOCVI, suggesting that improved soil structure enhances microbial-mediated aggregation and thus physically protects labile SOC from rapid microbial decomposition (Cui and Holden, 2015; Gillespie et al., 2014).

Our findings further highlight the necessity of optimizing microbial activities to stabilize SOC effectively. Excessively high specific microbial activities rapidly consume organic inputs, preventing their stabilization (Raiesi and Beheshti, 2014; Zhang et al., 2019b), whereas excessively low microbial activities hinder the transformation of labile C into more stable fractions (oPOC and MAOC) (Kivlin et al., 2013; Liang, 2020). Therefore, management strategies should focus on establishing optimal microbial activity through balanced soil chemical conditions (e.g., appropriate pH) and enhanced soil physical structure (e.g., increased pore volume). Considering urban climatic conditions, such as elevated MAT, is equally essential, given their strong influence on microbial metabolic rates.

Ultimately, our study emphasizes that merely increasing C inputs through multi-layer planting or organic amendments is insufficient to significantly reduce SOC vulnerability. Instead, integrated soil management strategies that simultaneously optimize soil physical structure (e.g., aeration-enhancing treatments), chemical conditions (avoiding excessive alkalinity or acidity), and microbial dynamics are essential. Practical approaches include adopting belt-type greenery configurations, retaining leaf litter on-site, applying organic fertilizers, and incorporating structural amendments such as biochar (Guimarães et al., 2013; Kim et al., 2021a; Lorenz and Lal, 2015; Malone et al., 2023; Zhang et al., 2022). Collectively, these measures represent a robust framework for enhancing SOC sequestration and long-term stability in artificially constructed urban green spaces.

5. Conclusions

This study investigated the mechanisms underlying low SOC storage in artificially constructed urban green spaces by integrating SOC fractionation analysis and microbial activity assessments as well as soil structural and chemical characterizations. Both the urban parks and tree-only roadside greenery had significantly lower SOC content than the grasslands, with the tree-only roadside greenery exhibiting the highest vulnerability index, SOCVI, due to severe compaction, low pore volume, and the absence of sustained organic inputs. These factors collectively constrained microbial activity and reduced SOC stabilization potential. Although the belt-type roadside greenery showed higher SOC content and some structural improvements relative to the tree-only roadside greenery, its SOCVI remained high. These findings underscore that enhancing C sequestration in artificially constructed urban soils requires not only expanding vegetation but also improving soil physical properties (e.g., ensuring adequate pore space, promoting aggregate formation), maintaining appropriate pH, and consistently providing organic inputs. This study offers foundational insights for developing management and policy measures to facilitate stable SOC accumulation in urban environments.

CRediT authorship contribution statement

Ye Lim Park: Writing – review & editing, Writing – original draft, Visualization, Validation, Methodology, Investigation, Formal analysis, Data curation, Conceptualization. **You Jin Kim:** Writing – review & editing, Validation, Methodology. **Jun Ge Hyun:** Validation, Methodology, Data curation. **Claire Chenu:** Writing – review & editing, Methodology. **Gayoung Yoo:** Writing – review & editing, Supervision, Resources, Project administration, Funding acquisition, Conceptualization.

Declaration of competing interest

The authors declare that they have no known competing financial interests or personal relationships that could have appeared to influence the work reported in this paper.

Acknowledgements

This work was carried out with the support of cooperative research program for agriculture science and technology development (project No. RS-2024-00395870) by Rural Development Administration, the Republic of Korea.

Appendix A. Supplementary data

Supplementary data to this article can be found online at https://doi.org/10.1016/j.geoderma.2025.117364.

Data availability

Data will be made available on request.

References

Act on Urban Parks and Green Areas, etc., 2005. https://elaw.klri.re.kr/eng_mobile/viewer.do?hseq=67756&type=part&key=33.
Bae, J., Ryu, Y., 2015. Land use and land cover changes explain spatial and temporal variations of the soil organic carbon stocks in a constructed urban park. Landsc. Urban Plan. 136, 57–67. https://doi.org/10.1016/j.landurbplan.2014.11.015.
Baldock, J., Beare, M., Curtin, D., Hawke, B., 2018. Stocks, composition and vulnerability to loss of soil organic carbon predicted using mid-infrared spectroscopy. Soil Res. 56 (5), 468–480.
Baldock, J., Sanderman, J., Macdonald, L., Puccini, A., Hawke, B., Szarvas, S., McGowan, J., 2013. Quantifying the allocation of soil organic carbon to biologically significant fractions. Soil Res. 51 (8), 561–576.
Balesdent, J., 1996. The significance of organic separates to carbon dynamics and its modelling in some cultivated soils. Eur. J. Soil Sci. 47 (4), 485–493.
Cambou, A., Shaw, R.K., Huot, H., Vidal-Beaudet, L., Hunault, G., Cannavo, P., Nold, F., Schwartz, C., 2018. Estimation of soil organic carbon stocks of two cities, New York City and Paris. Sci. Total Environ. 644, 452–464. https://doi.org/10.1016/j.scitotenv.2018.06.322.
Chen, J., Kim, H., Yoo, G., 2015. Effects of biochar addition on CO2 and N2O emissions following fertilizer application to a cultivated grassland soil. PLoS One 10 (5), e0126841. https://doi.org/10.1371/journal.pone.0126841.
Cotrufo, M.F., Ranalli, M.G., Haddix, M.L., Six, J., Lugato, E., 2019. Soil carbon storage informed by particulate and mineral-associated organic matter. Nat. Geosci. 12 (12), 989–994.
Cui, J., Holden, N.M., 2015. The relationship between soil microbial activity and microbial biomass, soil structure and grassland management. Soil Tillage Res. 146, 32–38.
Day, S.D., Bassuk, N.L., 1994. A review of the effects of soil compaction and amelioration treatments on landscape trees. Arboriculture & Urban Forestry (AUF) 20 (1), 9–17.
Del Galdo, I., Six, J., Peressotti, A., Francesca Cotrufo, M., 2003. Assessing the impact of land-use change on soil C sequestration in agricultural soils by means of organic matter fractionation and stable C isotopes. Glob. Chang. Biol. 9 (8), 1204–1213. https://doi.org/10.1046/j.1365-2486.2003.00657.x.
Delgado-Baquerizo, M., García-Palacios, P., Bradford, M.A., Eldridge, D.J., Berdugo, M., Sáez-Sandino, T., Liu, Y.-R., Alfaro, F., Abades, S., Bamigboye, A.R., 2023. Biogenic factors explain soil carbon in paired urban and natural ecosystems worldwide. Nat. Clim. Chang. 13 (5), 450–455.
Du, J., Yu, M., Cong, Y., Lv, H., Yuan, Z., 2022. Soil organic carbon storage in urban green space and its influencing factors: a case study of the 0–20 cm soil layer in Guangzhou City. Land 11 (9), 1484.
Dunn, C., Jones, T., Girard, A., Freeman, C., 2014. Methodologies for extracellular enzyme assays from wetland soils. Wetlands 34. https://doi.org/10.1007/s13157-013-0475-0.
Edmondson, J.L., Stott, I., Potter, J., Lopez-Capel, E., Manning, D.A., Gaston, K.J., Leake, J.R., 2015. Black carbon contribution to organic carbon stocks in urban soil. Environ. Sci. Tech. 49 (14), 8339–8346.
Fang, Y., Singh, B.P., Cowie, A., Wang, W., Arachchi, M.H., Wang, H., Tavakkoli, E., 2019. Balancing nutrient stoichiometry facilitates the fate of wheat residue-carbon in physically defined soil organic matter fractions. Geoderma 354, 113883.
Franzluebbers, A.J., 2020. Holding water with capacity to target porosity. Agric. Environ. Lett. 5 (1), e20029.
Freeman, C., Ostle, N., Kang, H., 2001. An enzymic'latch'on a global carbon store. Nature 409 (6817), 149.
Ghosh, S., Scharenbroch, B.C., Burcham, D., Ow, L.F., Shenbagavalli, S., Mahimairaja, S., 2016. Influence of soil properties on street tree attributes in Singapore. Urban Ecosystems 19, 949–967.
Gillespie, A., Diochon, A., Ma, B., Morrison, M., Kellman, L., Walley, F., Regier, T., Chevrier, D., Dynes, J., Gregorich, E., 2014. Nitrogen input quality changes the biochemical composition of soil organic matter stabilized in the fine fraction: a long-term study. Biogeochemistry 117, 337–350.

Gray, J., Karunaratne, S., Bishop, T., Wilson, B., Veeragathipillai, M., 2019. Driving factors of soil organic carbon fractions over New South Wales, Australia. Geoderma 353, 213–226.
Group, I.W., 2014. World reference base for soil resources 2014. International soil classification system for naming soils and creating legends for soil maps. (No Title).
Guimarães, R.M.L., Ball, B.C., Tormena, C.A., Giarola, N.F.B., da Silva, Á.P., 2013. Relating visual evaluation of soil structure to other physical properties in soils of contrasting texture and management. Soil Tillage Res. 127, 92–99.
Hernanz, J., Peixoto, H., Cerisola, C., Sánchez-Girón, V., 2000. An empirical model to predict soil bulk density profiles in field conditions using penetration resistance, moisture content and soil depth. J. Terramech. 37 (4), 167–184.
Hu, Y., Dou, X., Li, J., Li, F., 2018. Impervious surfaces alter soil bacterial communities in urban areas: a case study in Beijing China. Front. Microbiol. 9, 226.
Jeong, M., Bae, J., Yoo, G., 2024. Urban roadside greenery as a carbon sink: systematic assessment considering understory shrubs and soil respiration. Sci. Total Environ. 927, 172286. https://doi.org/10.1016/j.scitotenv.2024.172286.
Jian, S., Li, J., Wang, G., Kluber, L.A., Schadt, C.W., Liang, J., Mayes, M.A., 2020. Multi-year incubation experiments boost confidence in model projections of long-term soil carbon dynamics. Nat. Commun. 11 (1), 5864. https://doi.org/10.1038/s41467-020-19428-y.
Jim, C.Y., 1993. Soil compaction as a constraint to tree growth in tropical & subtropical urban habitats. Environ. Conserv. 20 (1), 35–49.
Jim, C.Y., 1998. Soil Characteristics and Management in an Urban Park in Hong Kong. Environ. Manag. 22 (5), 683–695.
Jim, C.Y., Ng, Y.Y., 2018. Porosity of roadside soil as indicator of edaphic quality for tree planting. Ecol. Eng. 120, 364–374.
kakao, 2025. Kakao Map. Seoul, Korea, Kakao. https://map.kakao.com.
Kim, E.-Y., Jung, K.-M., 2019. Analysis of health status of street trees and major affecting factors on Deogyeong-daero in Suwon. Journal of the Korean Society of Environmental Restoration Technology 22 (2), 49–57.
Kim, J., Rochefort, L., Hogue-Hugron, S., Alqulaiti, Z., Dunn, C., Pouliot, R., Jones, T.G., Freeman, C., Kang, H., 2021a. Water table fluctuation in peatlands facilitates fungal proliferation, impedes sphagnum growth and accelerates decomposition [original research]. Front. Earth Sci. 8. https://doi.org/10.3389/feart.2020.579329.
Kim, Y.J., Hyun, J., Yoo, S.Y., Yoo, G., 2021b. The role of biochar in alleviating soil drought stress in urban roadside greenery. Geoderma 404, 115223.
Kim, Y.J., Yoo, G., 2020. Suggested key variables for assessment of soil quality in urban roadside tree systems. J. Soil. Sediment. 21 (5), 2130–2140. https://doi.org/10.1007/s11368-020-02827-5.
Kivlin, S.N., Waring, B.G., Averill, C., Hawkes, C.V., 2013. Tradeoffs in microbial carbon allocation may mediate soil carbon storage in future climates. Front. Microbiol. 4, 261.
Korea Forest Service, 2007. Urban Forest Creation and Management Manual. U. F. P. D. Korea Forest Service.
Korea Forest Service, 2024. Statistics on the Status of Urban Forests in South Korea as of the End of 2023. https://www.forest.go.kr.
Korea Forest Service, M. o. E., Korea, 2020. Street Tree Planting and Management Manual.
Liang, C., 2020. Soil microbial carbon pump: mechanism and appraisal. Soil Ecol. Lett. 2 (4), 241–254.
Liang, M., Smith, N.G., Chen, J., Wu, Y., Guo, Z., Gornish, E.S., Liang, C., 2021. Shifts in plant composition mediate grazing effects on carbon cycling in grasslands. J. Appl. Ecol. 58 (3), 518–527.
Liu, X., Li, T., Zhang, S., Jia, Y., Li, Y., Xu, X., 2016. The role of land use, construction and road on terrestrial carbon stocks in a newly urbanized area of western Chengdu, China. Landsc. Urban Plan. 147, 88–95. https://doi.org/10.1016/j.landurbplan.2015.12.001.
Lorenz, K., Kandeler, E., 2005. Biochemical characterization of urban soil profiles from Stuttgart Germany. Soil Biology and Biochemistry 37 (7), 1373–1385.
Lorenz, K., Lal, R., 2009. Biogeochemical C and N cycles in urban soils. Environ. Int. 35 (1), 1–8.
Lorenz, K., Lal, R., 2015. Managing soil carbon stocks to enhance the resilience of urban ecosystems. Carbon Manage. 6 (1–2), 35–50.
Lugato, E., Lavallee, J.M., Haddix, M.L., Panagos, P., Cotrufo, M.F., 2021. Different climate sensitivity of particulate and mineral-associated soil organic matter. Nat. Geosci. 14 (5), 295–300. https://doi.org/10.1038/s41561-021-00744-x.
Malone, Z., Berhe, A.A., Ryals, R., 2023. Impacts of organic matter amendments on urban soil carbon and soil quality: a meta-analysis. J. Clean. Prod. 419, 138148.
Meyer, W.B., Turner, B.L., 1992. Human population growth and global land-use/cover change. Annu. Rev. Ecol. Syst. 39–61.
Midwood, A., Boutton, T., 1998. Soil carbonate decomposition by acid has little effect on δ13C of organic matter. Soil Biol. Biochem. 30 (10–11), 1301–1307.
Min, K., Freeman, C., Kang, H., Choi, S.U., 2015. The regulation by phenolic compounds of soil organic matter dynamics under a changing environment. Biomed Res. Int. 2015, 825098. https://doi.org/10.1155/2015/825098.
Ministry of Land, I. a. T., 2020. Korean National Atlas Vol. 2.
Miron, J., Millward, A.A., Vaziriyeganeh, M., Zwiazek, J.J., Urban, J., 2022. Winter climate variability, de-icing salt and streetside tree vitality. Front. Ecol. Evol. 10, 749168.
National Forestry Cooperative Federation. (2010). Tree Planting and Management Guidelines. https://www.nfcf.or.kr.
National Geographic Information Institutem, K. (2020). The National Atlas of Korea II. Retrieved 2025.02.27 from http://nationalatlas.ngii.go.kr.
Pan, P., Zhao, F., Ning, J., Zhang, L., Ouyang, X., Zang, H., 2018. Impact of understory vegetation on soil carbon and nitrogen dynamic in aerially seeded Pinus massoniana plantations. PLoS One 13 (1), e0191952.
Phillip, J.C., 1985. A description of urban soils and their desired characteristics. Arboriculture & Urban Forestry (AUF) 11 (11), 330–339. https://doi.org/10.48044/jauf.1985.071.
Poeplau, C., Kätterer, T., Leblans, N.I., Sigurdsson, B.D., 2017. Sensitivity of soil carbon fractions and their specific stabilization mechanisms to extreme soil warming in a subarctic grassland. Glob. Chang. Biol. 23 (3), 1316–1327.
Pouyat, R.V., Yesilonis, I.D., Nowak, D.J., 2006. Carbon storage by urban soils in the United States. J. Environ. Qual. 35 (4), 1566–1575. https://doi.org/10.2134/jeq2005.0215.
Raiesi, F., Beheshti, A., 2014. Soil specific enzyme activity shows more clearly soil responses to paddy rice cultivation than absolute enzyme activity in primary forests of northwest Iran. Appl. Soil Ecol. 75, 63–70. https://doi.org/10.1016/j.apsoil.2013.10.012.
Rillig, M.C., 2004. Arbuscular mycorrhizae, glomalin, and soil aggregation. Can. J. Soil Sci. 84 (4), 355–363.
Saraswati, S., Dunn, C., Mitsch, W.J., Freeman, C., 2016. Is peat accumulation in mangrove swamps influenced by the “enzymic latch” mechanism? Wetl. Ecol. Manag. 24 (6), 641–650. https://doi.org/10.1007/s11273-016-9493-z.
Scharenbroch, B.C., Catania, M., 2012. Soil quality attributes as indicators of urban tree performance. Arboriculture & Urban Forestry (AUF) 38 (5), 214–228.
Scharenbroch, B.C., Lloyd, J.E., Johnson-Maynard, J.L., 2005. Distinguishing urban soils with physical, chemical, and biological properties. Pedobiologia 49 (4), 283–296. https://doi.org/10.1016/j.pedobi.2004.12.002.
Sefati, Z., Khalilimoghadam, B., Nadian, H., 2019. Assessing urban soil quality by improving the method for soil environmental quality evaluation in a saline groundwater area of Iran. Catena 173, 471–480.
Seo, S., 1992. Grazing management. Journal of the Korean Society of Grassland Science 12 (3), 116–121.
Seto, K.C., Güneralp, B., Hutyra, L.R., 2012. Global forecasts of urban expansion to 2030 and direct impacts on biodiversity and carbon pools. Proc. Natl. Acad. Sci. 109 (40), 16083–16088.
Six, J., Elliott, E., Paustian, K., Doran, J., 1998. Aggregation and soil organic matter accumulation in cultivated and native grassland soils. Soil Sci. Soc. Am. J. 62 (5), 1367–1377.
Stursova, M., Sinsabaugh, R.L., 2008. Stabilization of oxidative enzymes in desert soil may limit organic matter accumulation. Soil Biol. Biochem. 40 (2), 550–553. https://doi.org/10.1016/j.soilbio.2007.09.002.
Suwon City, 2018. Suwon City Private Landscape Management Manual.
Tabachenik, D., Fidel, J., 2012. Structural equation modeling: guidelines for determining model fit. J. Bus Res. Methods 6 (5), 1–55.
Torbert, H.A., Wood, C., 1992. Effects of soil compaction and water-filled pore space on soil microbial activity and N losses. Commun. Soil Sci. Plant Anal. 23 (11–12), 1321–1331.
Troy, S.M., Lawlor, P.G., O’Flynn, C.J., Healy, M.G., 2013. Impact of biochar addition to soil on greenhouse gas emissions following pig manure application. Soil Biol. Biochem. 60, 173–181.
Truscott, A.-M., Palmer, S., McGowan, G., Cape, J., Smart, S., 2005. Vegetation composition of roadside verges in Scotland: the effects of nitrogen deposition, disturbance and management. Environ. Pollut. 136 (1), 109–118.
Viscarra Rossel, R.A., Lee, J., Behrens, T., Luo, Z., Baldock, J., Richards, A., 2019. Continental-scale soil carbon composition and vulnerability modulated by regional environmental controls. Nat. Geosci. 12 (7), 547–552.
Wright, S.F., Upadhyaya, A., 1998. A survey of soils for aggregate stability and glomalin, a glycoprotein produced by hyphae of arbuscular mycorrhizal fungi. Plant and Soil 198, 97–107.
Yang, J., Blondeel, H., Meeussen, C., Govaert, S., Vangansbeke, P., Boeckx, P., Lenoir, J., Orczewska, A., Ponette, Q., Hedwall, P.-O., Iacopetti, G., Brunet, J., De Frenne, P., Verheyen, K., 2022. Forest density and edge effects on soil microbial communities in deciduous forests across Europe. Appl. Soil Ecol. 179. https://doi.org/10.1016/j.apsoil.2022.104586.
Yoon, T.K., Seo, K.W., Park, G.S., Son, Y.M., Son, Y., 2016. Surface soil carbon storage in urban green spaces in three major South Korean cities. Forests 7 (6), 115.
Zhang, Q., Feng, J., Wu, J., Zhang, D., Chen, Q., Li, Q., Long, C., Feyissa, A., Cheng, X., 2019a. Variations in carbon-decomposition enzyme activities respond differently to land use change in central C hina. Land Degrad. Dev. 30 (4), 459–469.
Zhang, Q., Yu, R., Fu, S., Wu, Z., Chen, H.Y., Liu, H., 2019b. Spatial heterogeneity of heavy metal contamination in soils and plants in Hefei China. Scientific Reports 9 (1), 1049.
Zhang, X., Chen, X., Liu, M., Xu, Z., Wei, H., 2020. Coupled changes in soil organic carbon fractions and microbial community composition in urban and suburban forests. Sci. Rep. 10 (1), 15933.
Zhang, Z., Gao, X., Zhang, S., Gao, H., Huang, J., Sun, S., Song, X., Fry, E., Tian, H., Xia, X., 2022. Urban development enhances soil organic carbon storage through increasing urban vegetation. J. Environ. Manage. 312, 114922.
Zhao, D., Li, F., Yang, Q., Wang, R., Song, Y., Tao, Y., 2013. The influence of different types of urban land use on soil microbial biomass and functional diversity in Beijing China. Soil Use Manag. 29 (2), 230–239.